Volume 11
Number 23
21 June 2023
Pages 5035–5224

Journal of Materials Chemistry B

Materials for biology and medicine

rsc.li/materials-b

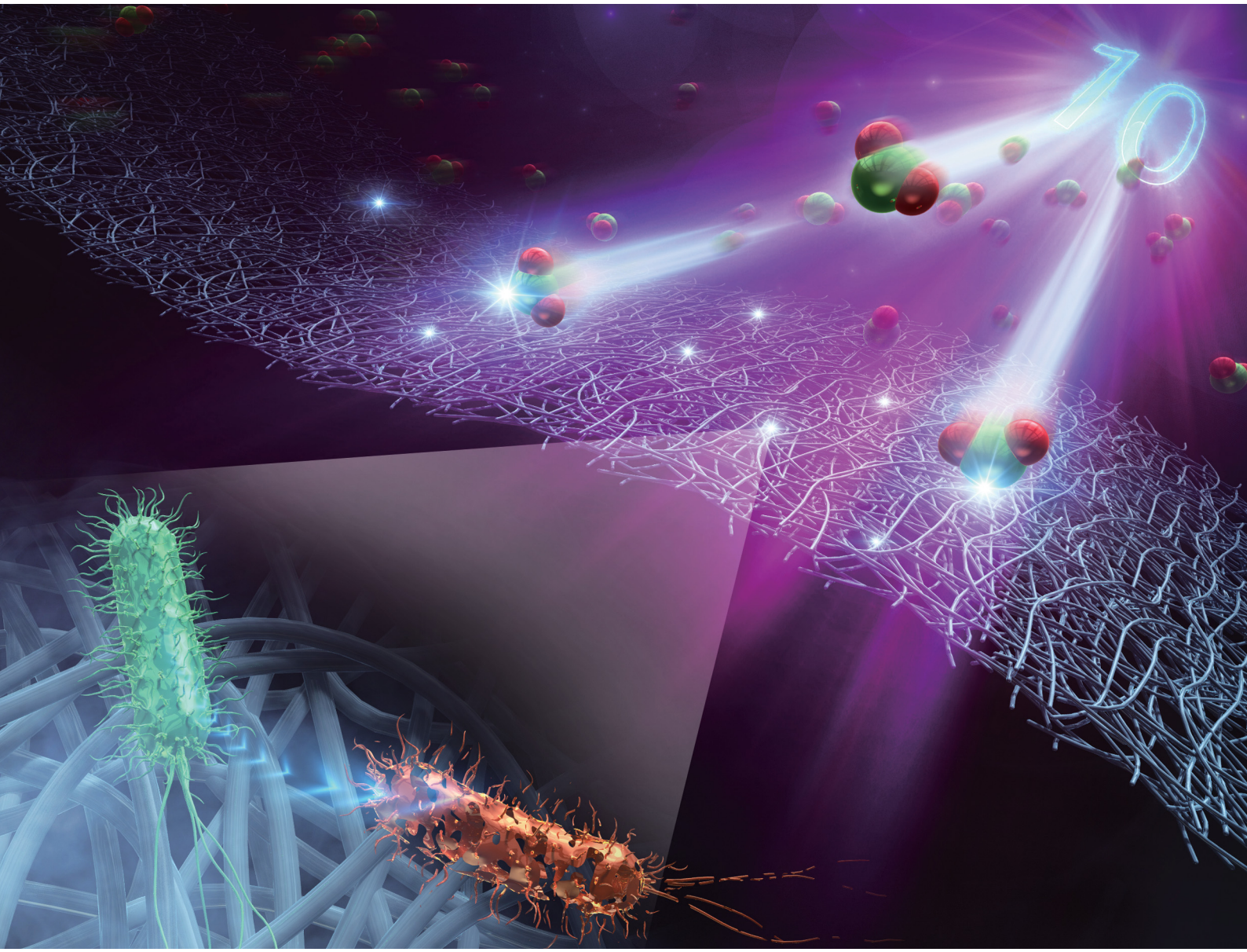

ISSN 2050-750X

ROYAL SOCIETY OF CHEMISTRY

PAPER

Haruyasu Asahara *et al.*

One-step antibacterial modification of polypropylene non-woven fabrics *via* oxidation using photo-activated chlorine dioxide radicals

10 YEARS ANNIVERSARY

Journal of Materials Chemistry B

ROYAL SOCIETY OF CHEMISTRY

PAPER

View Article Online
View Journal | View Issue

Cite this: J. Mater. Chem. B, 2023, 11, 5101

One-step antibacterial modification of polypropylene non-woven fabrics *via* oxidation using photo-activated chlorine dioxide radicals†

Keita Yamamoto, [a] Haruyasu Asahara, *[ab] Kazuo Harada, [a] Yuki Itabashi, [b] Kei Ohkubo [bc] and Tsuyoshi Inoue[ab]

Received 20th March 2023,
Accepted 10th May 2023

DOI: 10.1039/d3tb00586k

rsc.li/materials-b

In this study, we examined the modification of polypropylene non-woven fabrics (PP NWFs) *via* a one-step oxidation treatment using photo-activated chlorine dioxide radicals ($ClO_2^{\bullet}$). The oxidised PP NWFs exhibited excellent antibacterial activity against both *Escherichia coli* (Gram-negative) and *Staphylococcus aureus* (Gram-positive). The mound structure and antibacterial activity in the modified PP NWFs disappeared upon washing with a polar organic solvent. After washing, nanoparticles of around 80 nm in diameter were observed in the solution. The results of several mechanistic studies suggest that nanoparticles can contribute to the antimicrobial activity of oxidised PP NWFs.

Introduction

Polypropylene non-woven fabrics (PP NWFs) have been prevalent in industries such as medicine, sanitation and packaging, owing to their high mechanical strength and biocompatibility. However, in medical or sanitary applications, the presence of bacteria on the surface of PP NWFs can lead to serious problems, such as bacterial colonization and biofilm formation.[1] Hence, various approaches for bacterial inhibition have been investigated.[2–5] The antibacterial modification of device surfaces is a prevalent technique for preventing bacterial infections.[6] Various antibacterial agents, including antibiotics and antibacterial drugs, have been utilised as coatings on medical devices.[6]

Although many antibiotics and antibacterial drugs have been developed,[7,8] the emerging antimicrobial resistance (AMR) of bacteria has made the control and treatment of bacterial infections difficult.[9,10] For example, methicillin-resistant *Staphylococcus aureus* (MRSA) shows resistance against most β-lactam antibiotics, and the spread of MRSA in hospitals is an urgent problem.[11,12] Hence, an antibacterial strategy that is independent of antibiotics is a desirable solution.

Recently, antimicrobial peptides,[13,14] cationic compounds,[15–17] metal nanoparticles,[18,19] and polymer nanoparticles[20–22] have received considerable attention because of their broad-spectrum activities. They absorb on the membranes of bacterial cell and induce leakage of the cell contents. Membrane disruption is also effective against drug-resistant bacteria. For example, a surface modified with Ag nanoparticles has shown antibacterial activity against MRSA.[23]

By contrast, the direct modification of PP materials with antibacterial agents is difficult because they are hydrophobic and exhibit poor interactions with other molecules. Current methods for the antibacterial modification of PP NWFs are costly and require multiple steps, rendering them impractical for industrial use.[24–28] Hence, there is a need for an efficient and cost-effective method for the antibacterial modification of PP NWFs.

In recent years, our group has developed a surface-modification method for polymer materials that uses photo-activated chlorine dioxide radicals ($ClO_2^{\bullet}$).[29–32] The photo-activated $ClO_2^{\bullet}$ act as a strong oxidizing agent that is capable of cleaving C–H bonds, thus introducing oxygen-containing functional groups onto the polymer surface. This technique improves the hydrophilicity of PP films for better reactivity. In addition, owing to the gaseous oxidants used, our method is applicable to the oxidative modification of three-dimensional network structures such as PP NWFs.[32]

In this study, we found that oxidised PP NWFs exhibited excellent antibacterial properties against *Escherichia coli* (Gram-negative) and *Staphylococcus aureus* (Gram-positive). The modified PP NWFs were characterised using Fourier-transform infrared (FT-IR) spectroscopy, field-emission scanning electron microscopy (FE-SEM), X-ray photoelectron spectroscopy (XPS), and toluidine blue O (TBO) assays. The antibacterial mechanism of the modified PP NWFs was also investigated by

[a] Graduate School of Pharmaceutical Sciences, Osaka University, Yamada-oka 1-6, Suita, Osaka, 565-0871, Japan. E-mail: asahara@phs.osaka-u.ac.jp
[b] Institute for Open and Transdisciplinary Research Initiatives, Osaka University, Yamada-oka 1-6, Suita, Osaka, 565-0871, Japan
[c] Institute for Advanced Co-Creation Studies, Osaka University, Yamada-oka 1-6, Suita, Osaka, 565-0871, Japan

† Electronic supplementary information (ESI) available. See DOI: https://doi.org/10.1039/d3tb00586k

analysing the wash solvent used for the washing of PP NWF products. Unlike other methods, the as-described antibacterial modification process does not require antibiotics or antibacterial agents. In addition, the treatment described herein is convenient, is completed in one step, and is expected to be used practically.

Experimental section

Materials

Sodium chlorite ($NaClO_2$; 80%) was purchased from Sigma-Aldrich (St. Louis, MO, USA). Hydrochloric acid (HCl aq.) (35%), sodium hydroxide (NaOH aq.) (1 M), ethanol (99.5%), acetone, hexane, sodium chloride (NaCl), D(+)-glucose, agar, polysorbate 80, magnesium sulfate heptahydrate ($MgSO_4{\cdot}7H_2O$), Hipolypepton and chloroform-d ($CDCl_3$) (99.8%, containing 0.05 vol% TMS) were commercially obtained from FUJIFILM Wako Pure Chemical Co. (Tokyo, Japan). We also purchased toluidine blue O (TBO), sodium dodecyl sulfate (SDS), beef extract, casein peptone, tryptone and yeast extract from Nacalai Tesque (Kyoto, Japan); polypropylene non-woven fabric (PP NWF) was purchased from ASONE Co. (Tokyo, Japan); the bacterial strains were purchased from the NITE Biological Resource Centre (NBRC). *E. coli* (NBRC 3301, corresponding to NCIB 10083, NCTC 10538, DSM 11250) and *S. aureus* (NBRC 13276, corresponding to ATCC6538, NCTC 10788, DSM 799) were used for the antibacterial tests.

Oxidation of PP NWFs using photo-activated $ClO_2^{\bullet}$

The PP NWFs (50–60 mg; dimensions of 4 cm × 4 cm) were oxidised using $ClO_2^{\bullet}$ generated from an aqueous solution (20 mL) of $NaClO_2$ (200 mg) and 35% HCl aq. (100 μL), under irradiation with a 60 W LED lamp (λ = 365 nm, 5 mW cm^{-2}). A previously reported glassware system was used to carry out the oxidation of PP NWFs.[29–32] An aqueous solution of $ClO_2^{\bullet}$ was added to the outer moat of the glassware, while the sample was placed on the inner side. During the reaction, the samples were protected from direct UV irradiation using an aluminium sheet. The reaction was conducted for 20 min at 30 °C, 60 °C or 80 °C, and the oxidised samples were washed with distilled water and dried *in vacuo* – these are designated as Ox-30, Ox-60, and Ox-80, respectively (Scheme 1a).

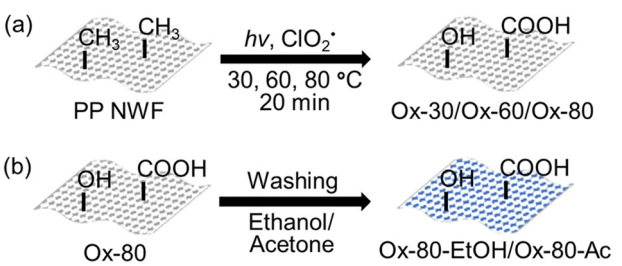

Scheme 1 (a) Oxidation of PP NWFs using photo-activated $ClO_2^{\bullet}$. (b) Solvent washing of oxidised PP NWFs.

Solvent washing of oxidised PP NWFs

Two solvents (ethanol (70%) and acetone) were used for washing. Solvent washing was performed by placing the oxidised PP NWF samples in each solvent and shaking for 1 min. The washed samples were then rinsed with distilled water three times, followed by drying *in vacuo*. The samples washed in ethanol and acetone, *e.g.*, for Ox-80, are denoted as Ox-80-EtOH and Ox-80-Ac, respectively (Scheme 1b).

Antibacterial testing of PP NWFs

Antibacterial testing of the PP NWF samples was performed according to the "absorption method" described in JIS L 1902 (corresponding to ISO 20743), a quantitative test to determine the antibacterial activity of textiles.[33] In this study, the sample weight was modified from 400 ± 50 mg to 14 ± 1 mg, the non-treated (control) and oxidised (test) PP NWF samples were cut into pieces (14 ± 1 mg; dimensions of 2 cm × 2 cm), and *E. coli* (Gram-negative) and *S. aureus* (Gram-positive) were selected as the test bacteria. The bacterial suspensions used to inoculate the samples were prepared as follows. One colony of bacteria was added to 20 mL of nutrient broth (NB) and incubated at 37 °C for 24 h (110 rpm). Next, 400 μL of the previous suspension was added to 20 mL of NB and incubated for 3 h at 37 °C (110 rpm). The bacterial concentration was measured and diluted with 1/20 NB (in distilled water) to approximately (1–3) × 10^5 colony-forming units mL^{-1} (CFU mL^{-1}). Then, each sample (six pieces each of the test sample and control sample) was inoculated with 200 μL of the prepared bacterial suspension. Three test samples and three control samples were mixed with 20 mL of physiological saline solution (8.5 g NaCl, 2.0 g polysorbate 80, in 1 L distilled water) immediately after inoculation. The remaining three test samples and three control samples were incubated at 37 °C for 20 h. Then, 20 mL of physiological saline solution was added to each sample and shaken. The pour-plate method was used to measure the number of live bacteria before and after incubation in each physiological saline solution used for washing. A series of 10-fold dilutions of the supernatant in physiological saline solution was performed, and 1 mL of each supernatant was plated on standard agar medium. The colonies in each plate were counted after 24 h of incubation at 37 °C. The antibacterial activity (A) was calculated using the following formula, and the values are defined in Table 1:

$$A = F - G$$

where F is the growth value of the control sample {*i.e.*, ($\log_{10}$ $CFU_{post\text{-}incubation}$) − ($\log_{10}$ $CFU_{pre\text{-}incubation}$)}, and G is the growth value of the test sample {*i.e.*, ($\log_{10}$ $CFU_{post\text{-}incubation}$) − ($\log_{10}$ $CFU_{pre\text{-}incubation}$)}. The percentage reduction in bacteria (%) after incubation for 20 h was calculated using the following formula:

$$(\text{Percentage reduction}) = (1 - 10^{-A}) \times 100\%$$

The *S. aureus* culture medium was prepared using 10 g of Hipolypepton, 2 g of yeast extract, 1 g of $MgSO_4{\cdot}7H_2O$, and 1 L

Table 1 Antibacterial activity rating associated with the percentage reduction in bacterial growth

Antibacterial activity (A)	Antibacterial efficiency	A	Percentage reduction (%)
$A \leqq 2$	No effect	1	90
$2 \leqq A < 3$	Good effect	2	99
		3	99.9
$A \geqq 3$	Excellent effect	4	99.99
		5	99.999

of distilled water instead of NB. Incubation was performed at 30 °C instead of 37 °C according to recommended culture conditions of the NBRC.

Surface characterization of PP NWFs

The surface functional groups of the PP NWF samples were determined *via* room-temperature FT-IR spectroscopy using a Spectrum TWO spectrophotometer (PerkinElmer, USA) with a diamond window. The surface elemental compositions and bonding states of the PP NWF samples were determined *via* XPS using an ESCA 3057 instrument (Ulvac-PHI, Japan) with a dual-anode Mg Kα source (1253.6 eV) operating at 400 W. A pass energy (PE) of 117.40 eV was used to acquire wide-range survey spectra, while a PE of 29.35 eV was used to acquire narrow C 1s spectra. The XPS data were analysed using Multi-Pak software (version 9). All spectra were calibrated with the hydrocarbon C 1s photoemission set at the 285.0 eV binding energy. The surface morphologies of the PP NWF samples were observed *via* FE-SEM using a JSM-F100 microscope (JEOL, Japan) set at 3.0 kV.

Quantification of surface carboxy groups on the PP NWFs

The surface carboxy (–COOH) groups of the PP NWF samples were quantified using the toluidine blue O (TBO) assay, based on the 1 : 1 formation of TBO with –COOH *via* electrostatic interactions.[34] First, PP NWF samples (2 cm × 2 cm) were incubated in 4 mL of the TBO solution (0.1% TBO in 1 mM NaOH) at 40 °C for 15 min (120 rpm). The samples were washed with 4 mL of 1 mM NaOH at 40 °C for 5 min with stirring (120 rpm). The washing process was repeated at least five times until the supernatant was clear. Finally, TBO was desorbed *via* incubation in 4 mL 20% SDS solution at 40 °C for 30 min (120 rpm). The TBO concentration in the SDS supernatant was calculated from the absorption at 630 nm using an ultraviolet-visible (UV-Vis) spectrophotometer V-750 (Jasco, Japan). The results were calculated as the average of three replicates.

Acetone washing of oxidised PP NWFs

First, 10 pieces of the PP NWFs samples (4 cm × 4 cm), including the non-treated, Ox-30, Ox-60, and Ox-80 samples, were prepared. The prepared samples were then placed in acetone (20 mL) and shaken for 1 min.

Optical microscopy observation of acetone washing solution

Optical microscopy of the acetone washing solution of the PP NWF samples was performed using a Spotlight 200i FT-IR microscope with a Spectrum Two spectrometer (PerkinElmer, USA).

Characterization of nanoparticles in the acetone washing solution of the PP NWFs

Optical microscopy measurements were performed using a BX53M optical microscope (OLYMPUS, Tokyo, Japan). The diameter of the nanoparticles was evaluated *via* dynamic light scattering (DLS) using an ELSZ-2 particle size analyser (Otsuka Electronics Co., Ltd, Japan). The samples for DLS measurements were prepared as follows. The PP NWF samples oxidised at 80 °C were placed in acetone and washed with distilled water. The acetone solution was shaken for 1 min, and the PP NWF samples were removed. The acetone solution was centrifuged at 12 000 rpm for 1 min for separation of the fibrous dispersion from the solution, and the supernatant including the nanoparticles was used for the DLS measurements. The zeta potential values of the nanoparticles in H_2O were measured using the ELSZ-2 instrument (Otsuka Electronics Co., Ltd, Japan). For the zeta potential measurements, the nanoparticle solution was prepared as follows. The Ox-80 samples were placed in acetone and then washed with distilled water. The acetone solution was shaken for 1 min and the PP NWFs were removed. The acetone solution was centrifuged at 12 000 rpm for 1 min for separation of the fibrous dispersion from the solution, and the supernatant including the nanoparticles was heated at 70 °C until the acetone had evaporated. The residue was dispersed in 60 μL of acetone followed by adding 3 mL of distilled water. Aqueous solutions were used for the zeta potential measurements. The results were calculated as the average of 10 replicates.

Results and discussion

Antibacterial testing of PP NWFs oxidised using photo-activated $ClO_2^{\bullet}$

We evaluated the antibacterial properties of the PP NWFs oxidised using photo-activated $ClO_2^{\bullet}$. The antibacterial properties of the as-prepared PP NWF samples, Ox-30 and Ox-80, were evaluated according to JIS L 1902.[33] The results are summarised in Table 2. Ox-80 showed a high antibacterial activity of over 3 in both *E. coli* and *S. aureus* (5.57 against *E. coli* and 5.12 against *S. aureus*) reduced by more than 99.9% compared with the non-treated PP NWFs, as per Table 1. Unlike Ox-80, Ox-30 showed an antibacterial activity of less than 2 (0.27 against *E. coli* and 1.45 against *S. aureus*), indicating that Ox-30 has no antibacterial activity against *E. coli* and *S. aureus*. We also evaluated the antibacterial activity of Ox-60 to examine the relationship between the antibacterial activity and the reaction temperature. As a result, Ox-60 showed antibacterial activity against *E. coli*,

Table 2 Results of antibacterial testing in Ox-30 and Ox-80

Bacteria		*E. coli*			*S. aureus*		
Sample		Non-treated	Ox-30	Ox-80	Non-treated	Ox-30	Ox-80
Log CFU	t = 0	4.58	4.70	4.65	4.72	4.78	4.72
	t = 20	7.80	7.65	2.30	8.02	6.63	2.90
A		—	0.27	5.57	—	1.45	5.12
Percentage reduction (%)		—	46.3	99.9997	—	96.5	99.9992

Table 3 Results of antibacterial testing in Ox-80-EtOH and Ox-80-Ac

Bacteria		*E. coli*		*E. coli*	
Sample		Non-treated	Ox-80-EtOH	Non-treated	Ox-80-Ac
Log CFU	t = 0	3.74	3.83	4.45	4.41
	t = 20	7.30	6.61	8.02	8.06
A		—	0.78	—	−0.08
Percentage reduction (%)		—	83.4	—	−20.2

and the bacterial growth was inhibited by 99.9% (Table S1, ESI†). Next, we performed an antibacterial test for Ox-80 against *E. coli* after solvent washing with 70% ethanol and acetone. Table 3 presents the antibacterial test results. The antibacterial activity of Ox-80-EtOH and Ox-80-Ac against *E. coli* was 0.78 and −0.08, respectively, indicating no antibacterial activity against *E. coli*, in contrast to Ox-80.

Characterization of oxidised PP NWFs

Chemical analyses and surface observations of the oxidised PP NWF samples were performed. First, the functional groups were characterised using FT-IR spectroscopy (Fig. 1, and Fig. S1, ESI†). In the oxidised samples, new peaks were observed at 1720 cm^{-1}, corresponding to the stretching of the carbonyl (C═O) groups.[32] Next, the oxidised PP NWF samples were washed with 70% ethanol and acetone. After washing, the characteristic carbonyl peaks at 1720 cm^{-1} were diminished, especially in Ox-80, indicating that the newly incorporated carbonyl groups were unstable in polar organic solvents.

The FE-SEM images obtained (Fig. 2) revealed mound structures on the surface of Ox-80, as previously reported.[32] After washing with ethanol and acetone, the mounds on Ox-80 disappeared, indicating that the surface deposits were washed away by polar organic solvents. Considering the diminished

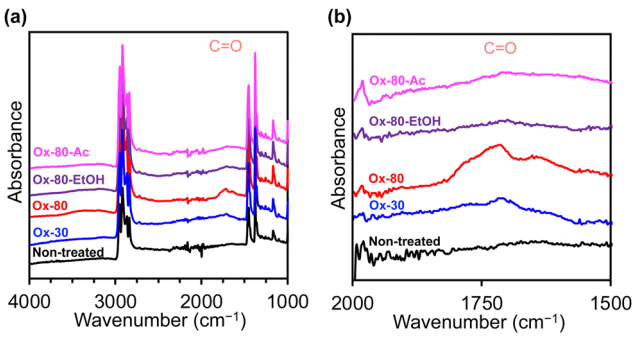

Fig. 1 FT-IR spectra of PP NWFs over wavenumber ranges of (a) 4000–1000 cm^{-1} and (b) 2000–1500 cm^{-1}: non-treated (black), Ox-30 (blue), Ox-80 (red), Ox-80-EtOH (purple), and Ox-80-Ac (pink).

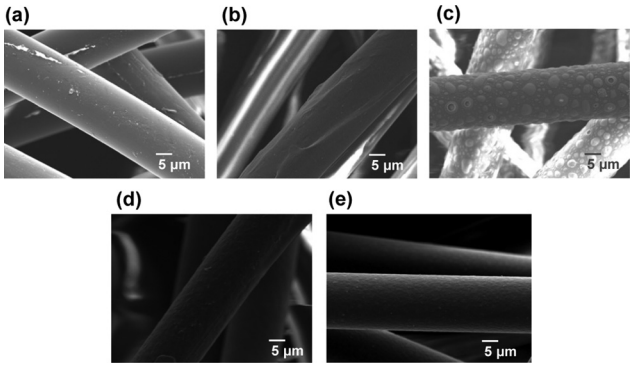

Fig. 2 FE-SEM images of the PP NWF samples: (a) non-treated, (b) Ox-30, (c) Ox-80, (d) Ox-80-EtOH, and (e) Ox-80-Ac.

1720 cm^{-1} peaks, the surface deposits are presumed to be rich in carbonyl groups.

To further characterize the surface of the PP NWF samples, the surface elemental and chemical compositions were determined *via* XPS (Fig. S2 in the ESI†: the wide-scan XPS spectra). Only carbon was detected in the control samples, whereas Ox-30 and Ox-80 contained 15.1% and 12.0% oxygen, respectively (Table 4). By contrast, Ox-80-EtOH contained 5.0% oxygen, indicating a decreased oxygen ratio after washing with ethanol. To further our understanding, the C 1s XPS spectra of the PP NWF samples were analysed. The C 1s XPS spectra exhibit five distinct peaks at 285.0, 286.3, 287.0, 288.3, and 289.1 eV, which are attributed to C–C, C–O, C–Cl, C–Cl_2/C═O, and –COO groups, respectively (Fig. S3 in ESI†). Table 5 lists the ratios of the functional groups. In Ox-30 and Ox-80, the ratio of –COO groups was 2.8% and 4.2%, respectively, suggesting that more carboxy groups were introduced to the PP NWFs during

Table 4 Surface elemental compositions (%) of the PP NWF samples, as measured *via* XPS

	C	N	O	Cl
Non-treated	100.0	—	—	—
Ox-30	69.7	—	15.1	15.1
Ox-80	77.3	—	12.0	10.7
Ox-80-EtOH	90.5	—	5.0	4.5

Table 5 Ratios of carbon-containing functional groups (%) on the PP NWF samples at specified peaks (eV), as determined *via* C 1s XPS

	C–C (285.0)	C–O (286.3)	C–Cl (287.0)	C–Cl_2/C═O (288.3)	COO (289.1)
Non-treated	100.0	—	—	—	
Ox-30	69.7	—	15.1	15.1	
Ox-80	77.3	—	12.0	10.7	
Ox-80-EtOH	90.5	—	5.0	4.5	

Table 6 Amount of adsorbed TBO for quantification of the surface –COOH groups in the PP NWF samples (n = 3)

Sample	TBO (μmol g^{-1})
Non-treated	0.5 ± 0.2
Ox-30	2.7 ± 0.1
Ox-80	10.0 ± 1.0
Ox-80-EtOH	0.8 ± 0.1
Ox-80-Ac	1.2 ± 0.1

oxidation at 80 °C than at 30 °C. In Ox-80-EtOH, the ratio of –COO groups was only 0.1%, which is consistent with the decreased intensity of the carbonyl peak at 1720 cm^{-1} after ethanol washing.

The C 1s XPS spectra showed a decrease in carboxy groups upon washing with polar organic solvents. Here, we quantified the surface carboxy groups per unit mass of PP NWFs using the toluidine blue O (TBO) assay. Table 6 present the results of the TBO assay (the data are shown in Fig. S4 (ESI†)). The non-treated samples exhibited limited TBO adsorption, whereas the oxidised samples exhibited good TBO absorption. The calculated surface carboxy groups on the non-treated, Ox-30, and Ox-80 samples were 0.5 ± 0.2, 2.7 ± 0.1, and 10.0 ± 1.0 μmol g^{-1}, respectively. By contrast, the calculated surface carboxy groups on Ox-80-EtOH and Ox-80-Ac were 0.8 ± 0.1 and 12.0 ± 0.1 μmol g^{-1}, respectively. These results suggest a decrease in the surface carboxy groups after ethanol washing.

Antibacterial mechanism of oxidised PP NWFs

In recent years, antibacterial nanoparticles with various surface potential values have been reported.[20,21,35] In particular, Sarian *et al.* reported negatively charged cyanoacrylate nanoparticles (20–250 nm) that show a growth inhibitory effect against Gram-positive and Gram-negative bacteria.[20] The authors considered that the antibacterial activity was derived from disruption of the bacterial membrane and the subsequent generation of reactive oxygen species (ROS) *via* physical interactions.[20] The cyanoacrylate nanoparticles also induced disorder of the cell walls and inhibited growth in green microalgae, such as *Chlamydomonas reinhardtii*,[36,37] and several non-green algae.[38] Here, we considered the formation of nanoparticles during oxidation with photo-activated $ClO_2^{\bullet}$ as a factor that governs the antibacterial activity. The experimental results showed that Ox-80 exhibited excellent antibacterial activity, whereas Ox-80-EtOH and Ox-80-Ac did not, indicating that washing with polar organic solvents affected the antibacterial activity. The physical and chemical characteristics of the samples washed with polar organic solvents were examined to identify their antibacterial mechanism. Acetone was selected as the washing solvent because it has a lower boiling point than ethanol. The soluble and insoluble components of the acetone washing solution of Ox-80 were analysed. The results from the examination of the acetone-soluble components are shown in the ESI.†

Ten pieces of the Ox-80 sample (571.2 mg) were prepared and washed with acetone (20 mL). After washing and drying, the weight decreased to 563.5 mg, which is a 1.35% loss (7.7 mg). Ten pieces of the non-treated and Ox-30 samples were also washed with acetone. By contrast, the weight loss from acetone washing in the non-treated and Ox-30 samples was only 0.04% and 0.34%, respectively. The difference in weight change is consistent with the disappearance of the surface mounds after washing with a polar solvent, as shown in Fig. 2. Therefore, we predict that this weight change is due to cleavage of the PP main chains during oxidation to form smaller products that are acetone-soluble.

The acetone-insoluble components of the washing solution were also examined. Fibrous dispersions were observed in the acetone solutions of both the non-treated and Ox-80 samples (Fig. S5 (ESI†)). An optical microscope (Spotlight 200i) was used to for further examination, and revealed that PP fibers and middle-sized particles (~50 μm) are present in both samples (Fig. S6 and S7, ESI†). By contrast, small particles (<1 μm) were observed only in the Ox-80 sample (Fig. S6, ESI†). Dynamic light scattering (DLS) measurements were carried out, and it was determined that 94.4% of the small Ox-80 particles were distributed in the range of 65–140 nm (Fig. 3). The average diameter of the nanoparticles in this area was 82.6 ± 16.1 nm.

The zeta potential of nanoparticles in H_2O was −25.0 ± 2.7 mV. Here, we predict that the ~80 nm nanoparticles found on the PP fibers are related to its antibacterial activity, and that the oxidation reaction temperature affects the number of

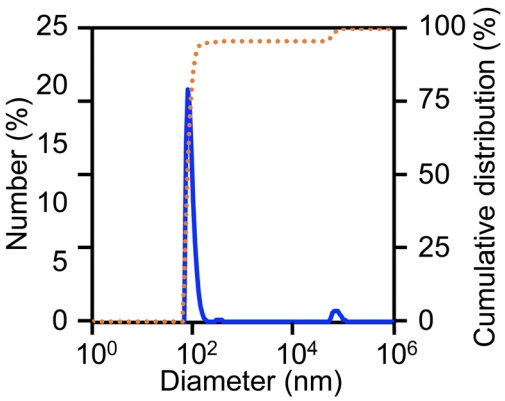

Fig. 3 Diameter of nanoparticles as measured using DLS. The nanoparticles were extracted from the Ox-80 PP NWF samples using acetone. The blue solid line and the orange dotted line show the number (%) and the cumulative distribution (%), respectively.

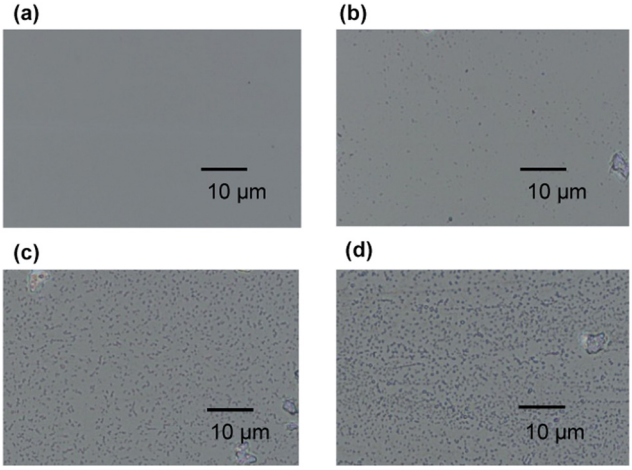

Fig. 4 Optical microscopy images (×5000) of the acetone washing solution after washing the PP NWF samples: (a) non-treated, (b) Ox-30, (c) Ox-60, and (d) Ox-80.

nanoparticles formed on the PP fibers. To examine the relative number of nanoparticles, an optical microscope (BX53M) was used to observe the acetone washing solution of the PP NWF samples (non-treated, Ox-30, Ox-60, and Ox-80 samples). The PP NWF samples were prepared (4 cm × 4 cm; 55 ± 1 mg) and washed with 5 mL of acetone. Fig. 4 and Fig. S8 (ESI†) show the optical microscopy images of the acetone washing solutions. In the non-treated and Ox-30 samples, nanoparticles were hardly observed, whereas nanoparticles were observed at high density in the Ox-60 and Ox-80 samples, indicating that more nanoparticles were formed through oxidation at 60 °C and 80 °C compared with at 30 °C.

Based on these results, we suggest that the excellent antibacterial activity of the Ox-60 and Ox-80 PP NWFs can be attributed to the ∼80 nm nanoparticles formed during oxidation. There was a correlation between the antibacterial activity of the PP NWFs and the number of nanoparticles formed, and the acetone extracts of Ox-80 that included the nanoparticles showed the growth inhibition of *E. coli* (ESI); however, other factors could not be ruled out in this experiment. Whether the nanoparticles themselves impart antibacterial properties to the PP NWFs remains to be examined. Further investigations focusing on the antibacterial mechanism of nanoparticles are ongoing in our laboratory.

In medical situations, PP NWFs are used for disposable equipment, such as masks or gowns, because of their low cost. Hence, the antibacterial modification method for PP NWFs is expected to be inexpensive for practical and industrial use. By contrast, our modification method has an advantage regarding the cost. The $ClO_2^•$ utilized for our modification can be prepared simply using inexpensive reagents ($NaClO_2$ and HCl). In addition, our method requires only a single step and the modification effects are stable in air and H_2O (Fig. S9, ESI†). Considering the above, our findings are of scientific and practical interest.

Conclusions

We demonstrated that PP NWFs oxidised at 80 °C using photo-activated $ClO_2^•$ exhibit excellent antibacterial activity against *E. coli* (Gram-negative) and *S. aureus* (Gram-positive). To investigate the underlying mechanism of antibacterial activity, we analysed the polar organic solvents used to wash the oxidised PP NWFs. We found nanoparticles of ∼80 nm in diameter in the solvent, particularly when the oxidation step was carried out at high temperature (60 °C and 80 °C). Our findings suggest that the nanoparticles are formed during oxidation, and are involved in the antibacterial properties of the oxidised PP NWFs. The detailed structure of the nanoparticles, their mechanism of antimicrobial activity, and the long-term stability of the oxidized non-woven fabrics are still under investigation and will be reported in the near future.

Conflicts of interest

There are no conflicts to declare.

Acknowledgements

This work was supported by the JSPS KAKENHI Grant JP20K05606 to H.A., the NEDO (New Energy and Industrial Technology Development Organization) grant 17101509-0 to H.A., and the JST OPERA (Open Innovation with Enterprises, Research Institute, and Academia) grant JPMJOP1861 to T.I.

Notes and references

1 S. Doron and S. L. Gorbach, *Int. Encycl. Public. Health*, 2008, 273–282.
2 B. Cao, X. Lyu, C. Wang, S. Lu, D. Xing and X. Hu, *Biomaterials*, 2020, **262**, 120341.
3 Q. Zhou, X. Lyu, B. Cao, X. Liu, J. Liu, J. Zhao, S. Lu, M. Zhan and X. Hu, *Front. Chem.*, 2021, **9**, 755419.
4 Z. Wang, M. Zhan and X. Hu, *Chem. - Eur. J.*, 2022, **28**, e202200042.
5 I. Mukherjee, A. Ghosh, P. Bhadury and P. De, *J. Mater. Chem. B*, 2019, **7**, 3007–3018.
6 I. Francolini, C. Vuotto, A. Piozzi and G. Donelli, *APMIS*, 2017, **125**, 392–417.
7 K. M. G. O. Connell, J. T. Hodgkinson, H. F. Sore, M. Welch, G. P. C. Salmond and D. R. Spring, *Angew. Chem., Int. Ed.*, 2013, **52**, 10706–10733.
8 M. Miethke, M. Pieroni, T. Weber, M. Brönstrup, P. Hammann, L. Halby, P. B. Arimondo, P. Glaser, B. Aigle, H. B. Bode, R. Moreira, Y. Li, A. Luzhetskyy, M. H. Medema, J.-L. Pernodet, M. Stadler, J. R. Tormo, O. Genilloud, A. W. Truman, K. J. Weissman, E. Takano, S. Sabatini, E. Stegmann, H. Brötz-Oesterhelt, W. Wohlleben, M. Seemann, M. Empting, A. K. H. Hirsch, B. Loretz, C.-M. Lehr, A. Titz, J. Herrmann, T. Jaeger, S. Alt, T. Hesterkamp, M. Winterhalter, A. Schiefer, K. Pfarr, A. Hoerauf, H. Graz, M. Graz, M. Lindvall, S. Ramurthy, A. Karlén, M. van Dongen, H. Petkovic, A. Keller, F. Peyrane,

S. Donadio, L. Fraisse, L. J. V. Piddock, I. H. Gilbert, H. E. Moser and R. Müller, *Nat. Rev. Chem.*, 2021, **5**, 726–749.
9 G. Sun, Q. Zhang, Z. Dong, D. Dong, H. Fang, C. Wang, Y. Dong, J. Wu, X. Tan, P. Zhu and Y. Wan, *Front. Public Health*, 2022, **10**, 1002015.
10 R. Urban-Chmiel, A. Marek, D. Stępień-Pyśniak, K. Wieczorek, M. Dec, A. Nowaczek and J. Osek, *Antibiotics*, 2022, **11**, 1079.
11 A. S. Lee, H. de Lencastre, J. Garau, J. Kluytmans, S. Malhotra-Kumar, A. Peschel and S. Harbarth, *Nat. Rev. Dis. Primers*, 2018, **4**, 18033.
12 P. Nandhini, P. Kumar, S. Mickymaray, A. S. Alothaim, J. Somasundaram and M. Rajan, *Antibiotics*, 2022, **11**, 606.
13 Y. J. Xi, T. Song, S. Y. Tang, N. S. Wang and J. Z. Du, *Biomacromolecules*, 2016, **17**, 3922–3930.
14 S. Rotem, I. S. Radzishevsky, D. Bourdetsky, S. Navon-Venezia, Y. Carmeli and A. Mor, *FASEB J.*, 2008, **22**, 2652–2661.
15 A. Morandini, E. Spadati, B. Leonetti, R. Sole, V. Gatto, F. Rizzolio and V. Beghetto, *RSC Adv.*, 2021, **11**, 28092–28096.
16 K. M. Docherty and C. F. Kulpa Jr., *Green Chem.*, 2005, **7**, 185–189.
17 I. Mukherjee, A. Ghosh, P. Bhadury and P. De, *ACS Omega*, 2017, **2**, 1633–1644.
18 K. Kalishwaralal, S. BarathManiKanth, S. R. K. Pandian, V. Deepak and S. Gurunathan, *Colloids Surf., B*, 2010, **79**, 340–344.
19 G. Ren, D. Hu, E. W. Cheng, M. A. Vargas-Reus, P. Reip and R. P. Allaker, *Int. J. Antimicrob. Agents*, 2009, **33**, 587–590.
20 F. D. Sarian, K. Ando, S. Tsurumi, R. Miyashita, K. Ute and T. Ohama, *Membranes*, 2022, **12**, 782.
21 K. Suga, M. Murakami, S. Nakayama, K. Watanabe, S. Yamada, T. Tsuji and D. Nagao, *ACS Appl. Bio Mater.*, 2022, **5**, 2202–2211.
22 C. Wang, W. Zhao, B. Cao, Z. Wang, Q. Zhou, S. Lu, L. Lu, M. Zhan and X. Hu, *Chem. Mater.*, 2020, **32**, 7725–7738.
23 J. Wang, J. Li, G. Guo, Q. Wang, J. Tang, Y. Zhao, H. Qin, T. Wahafu, H. Shen, X. Liu and X. Zhang, *Sci. Rep.*, 2016, **6**, 32699.
24 Z. Xin, S. Du, C. Zhao, H. Chen, M. Sun, S. Yan, S. Luan and J. Yin, *Appl. Surf. Sci.*, 2016, **365**, 99–107.
25 Y. Ma, N. Wisuthiphaet, H. Bolt, N. Nitin, Q. Zhao, D. Wang, B. Pourdeyhimi, P. Grondin and G. Sun, *ACS Biomater. Sci. Eng.*, 2021, **7**, 2329–2336.
26 N. Prorokova, V. Istratkin, T. Kumeeva, S. Vavilova, A. Kharitonov and V. Bouznik, *RSC Adv.*, 2015, **5**, 44545–44549.
27 D. Marković, H. Tseng, T. Nunney, M. Radoičić, T. Ilic-Tomic and M. Radetić, *Appl. Surf. Sci.*, 2020, **527**, 146829.
28 Y. Xu, L. Tian, J. Li, X. Lv, F. Li, L. Sun, L. Niu, X. Li and Z. Zhang, *Sci. Rep.*, 2022, **12**, 13206.
29 K. Ohkubo and K. Hirose, *Angew. Chem., Int. Ed.*, 2018, **57**, 2126–2129.
30 K. Ohkubo, H. Asahara and T. Inoue, *Chem. Commun.*, 2019, **55**, 4723–4726.
31 Y. Jia, J. Chen, H. Asahara, T. Asoh and H. Uyama, *ACS Appl. Polym. Mater.*, 2019, **1**, 3452–3458.
32 K. Yamamoto, H. Asahara, H. Moriguchi and T. Inoue, *Polym. J.*, 2023, **55**, 599–605.
33 JIS L 1902. Japanese industry standard for testing antibacterial activity and efficiency in textile products.
34 S. Sano, K. Kato and Y. Ikada, *Biomaterials*, 1993, **14**, 817–822.
35 C. Fang, L. Kong, Q. Ge, W. Zhang, X. Zhou, L. Zhang and X. Wang, *Polym. Chem.*, 2019, **10**, 209–218.
36 D. Widyaningrum, D. Iida, Y. Tanabe, Y. Hayashi, S. D. Kurniasih and T. Ohama, *J. Phycol.*, 2019, **55**, 118–133.
37 A. J. S. Al-Azab, Y. Aoki, F. D. Sarian, Y. Sori, D. Widyaningrum, T. Yamasaki, F. Kong and T. Ohama, *Algal Res.*, 2022, **68**, 102884.
38 A. J. S. Al-Azab, D. Widyaningrum, H. Hirakawa, Y. Hayashi, S. Tanaka and T. Ohama, *Algal Res.*, 2021, **54**, 102191.